Effects of a rapid depressurization in a salt cavern

P. Bérest & H. Djizanne
LMS, Ecole Polytechnique ParisTech, Palaiseau, France

B. Brouard
Brouard Consulting, Paris, France

G. Hévin
Storengy, Bois-Colombes, France

ABSTRACT: Rapid gas depressurization leads to gas cooling followed by slow gas warming when the cavern is kept idle. Gas temperature drop depends upon withdrawal rate and cavern size. Thermal tensile stresses, resulting from gas cooling, may generate frac-tures at the wall and roof of a salt cavern. These fractures are perpendicular to the cavern wall; in most cases their depth of penetration is small. The distance between two parallel fractures becomes larger when fractures penetrate deeper in the rock mass, as some fractures stop growing. These conclusions can be supported by numerical computations based on fracture mechanics. Salt slabs are created. These slabs remain strongly bounded to the rock mass and it is believed that in many cases their weight is not large enough to allow them to break off the cavern wall. However, depth of penetration of the fractures must be computed to prove that they cannot be a concern from the point of view of cavern tightness.

1 INTRODUCTION

Gas storage caverns used to be developed mainly for seasonal storage, with one cycle per year and a moderate pressure rate between the maximum and minimum operation pressure (1 MPa/day often was a maximum depressurization rate). However, the needs of energy traders are prompting change toward more aggressive operating modes. Typically, high-deliverability caverns (HFCGSC) can be emptied in 10 days and refilled in 30 days or less. At the same time, Compressed Air Energy Storage (CAES) is experiencing a rise in interest. They are designed to deliver full-power capacity in a very short time period.

Both types of facilities imply high gas-production rates and multiple yearly pressure cycles. This cycled mode of operation raises questions regarding frequently repeated, extreme, mechanical and thermal loading.

2 TEMPERATURE CHANGES IN A GAS CAVERN

2.1 *Convection in a gas-filled cavern*

Gas density is small (50 to 200 kg/m^3) and in a gas cavern, pressure is almost uniform. Temperature distribution raises a more difficult problem. In a salt formation, rock thermal conductivity is K_R = 5 to 6 W/m/°C and the geothermal gradient typically is G = 1.5 to 1.8 °C/100 m. However, as gas (or liquid) conductivity, or K_F, is significantly smaller than rock conductivity, or K_R, the geothermal gradient at rest should be larger in the cavern fluid (G_c) than in the rock mass. For instance, in a spherical cavern it is $G_c = 3K_RG/(K_F + 2K_R)$. In fact, gas effectively is stirred by thermal convection: temperature is warmer at the cavern bottom, gas is lighter, gas is driven upward by gravity forces and convection cells appear. However, natural convection only occurs when the geothermal gradient is larger than a certain threshold, the *adiabatic* gradient (G_{ad}). Considering the simple example of a dry gas $G_{ad} = g/C_P$ where g = 10 m/s^2 is the gravity acceleration, and C_P is the specific heat of gas (when pressure is kept constant). For natural gas, C_P = 2345 J/kg/°C and for air, C_P = 1000 J/kg/°C. In other words $G > G_{ad}$ and, in principle, convection must appear in any cavern. However, G is not *much* larger than G_{ad}, and convection can be impeded in some cases — for instance, when warm gas is injected at the cavern top, when cold brine is left at the cavern bottom at the end of the leaching period, or when gas is cooled to a temperature colder than the temperature of the brine left at the cavern bottom. Examples can be found in Quast, 1983, Fosse & Røvang, 1998, Krieter et al., 1998, Kneer et al., 2003, Klafki et al., 2003 and Skaug et al., 2010.

When thermal convection develops, it is extremely effective. Dimensional analysis shows that con-

vection is governed by the Prandtl number ($Pr = \nu/k$, ν = kinematic viscosity, k = gas thermal diffusivity) and the Grashof number ($Gr = g\alpha Ga^4/\nu^2$), where a is the cavern characteristic length, α is the gas thermal expansion coefficient. The Grashof number is quite high in a large cavern, and turbulent convection develops. In a *brine*-filled cavern $G_{ad} = \alpha_b Tg/C_P$ = 0.035 °C/100 m is much smaller than the geothermal gradient G: onset of convection is certain (α_b is the brine thermal expansion coefficient).

2.2 *Heat balance equation*

When it is assumed that gas absolute temperature, T, and pressure, P, are almost uniform throughout the entire cavern, the heat balance equation can be written (ATG, 1986):

$$m\left(C_P\dot{T} + \frac{1}{\rho^2}T\frac{\partial\rho}{\partial T}\bigg|_P\dot{P}\right) = L\dot{C} + <\dot{m}>C_P(T_{inj} - T) - \int K_R\frac{\partial T_R}{\partial n}da \qquad (1)$$

where ρ, m are gas density and mass, respectively; T_R is rock temperature. The gas state-equation can be written $P = \rho rTZ(P,T)$, where $Z = Z(P, T)$ is the gas compressibility factor. Kinetic energy is neglected. The left-hand side reflects the changes in internal energy minus the work of the external forces. The right-hand side is the sum of: the heat generated during condensation and vaporization of water vapor (This term is neglected in this paper; C is the mass of water vapor.) plus the enthalpy flux that enters the cavern during gas injection (T_{inj} is the temperature of the injected gas; this flux vanishes when no gas is injected in the cavern, $\dot{m} < 0$ (withdrawal) or $\dot{m} = 0$ (standstill) plus the heat flux crossing the cavern walls. The evolution of temperature in the rock mass is governed by thermal conduction. Generally speaking, penetration of temperature changes in the rock mass is slow. For instance, when a cold gas temperature has been kept constant at the cavern wall during a t-long period of time, the rock temperature is changed significantly in a domain at cavern wall with a thickness of $d = \sqrt{k_R t}$ or $d \approx 1\,\mathrm{m}$ after t = 4 days, where $k_R \approx 3\times10^{-6}\,\mathrm{m^2/s}$ is the rock thermal diffusivity. In consequence, when a rapid depressurization is considered, from the point of view of thermal conduction, the surface S of the cavern can be considered as a flat surface (Krieter, 2011, and Crotogino et al, 2001).

2.3 *Gas withdrawal*

In the following, simplifying assumptions are made. The boundary condition at cavern wall raises a difficult problem: it is likely that gas temperature gradient is large in a thin boundary layer at cavern wall whose thickness depends on wall roughness and on the rate of the convective gas flow. For simplicity, it is assumed that rock temperature at cavern wall equals gas temperature. Only gas withdrawal is considered, $\dot{m} < 0$. The gas is ideal and its state equation is $P = \rho rT$. Cavern compressibility is quite small when compared to gas compressibility and the cavern volume, or $V_0 = m/\rho$, is assumed to remain constant. The "flat surface" assumption is accepted and Equation (1) then can be re-written:

$$m(t)C_v\dot{T}(t) - \dot{m}(t)rT(t) = -SK_R\int_0^t\frac{\dot{T}(\tau)}{\sqrt{k_R(t-\tau)}}d\tau \qquad (2)$$

$r = C_p - C_v$ is the difference between the specific heats of the gas at constant pressure and constant volume, respectively. In an actual cavern, the right-hand side of (2), or the heat flux crossing the cavern walls, cannot be neglected and the "adiabatic" solution, or $T/T_0 = (m/m_0)^{\gamma-1}$, where $\gamma = C_p/C_v$, does not apply. Dimensional analysis proves that, following withdrawal of a certain amount of gas (in % of the total gas inventory), gas temperature at the end of the withdrawal is lower when the withdrawal rate is faster or when the cavern is bigger.

2.4 Example

Crotogino et al (2001) described a withdrawal test performed in a Huntorf (Germany) CAES cavern. We did not try to backcalculate cavern gas evolution; we selected a somewhat similar example which is represented on Figure 1. Cavern volume is 170 000 m^3 and cavern walls overall surface is 10 800 m^2. Cavern pressure is lowered from 7 MPa to 4.3 MPa. Rock mass virgin temperature is 35°C. The following values were selected: γ = 1.408, and C_v = 719 J/kg/°C. Air flow rate is 108 kg/s during 5 hours and decreases linearly to 30 kg/s during the following 11 hours. Note that slightly before the end of the withdrawal phase (hour 11), gas temperature starts warming, as heat flux from the rock mass becomes quite fast, a phenomenon actually observed in the Huntorf cavern by Crotogino et al. (2001).

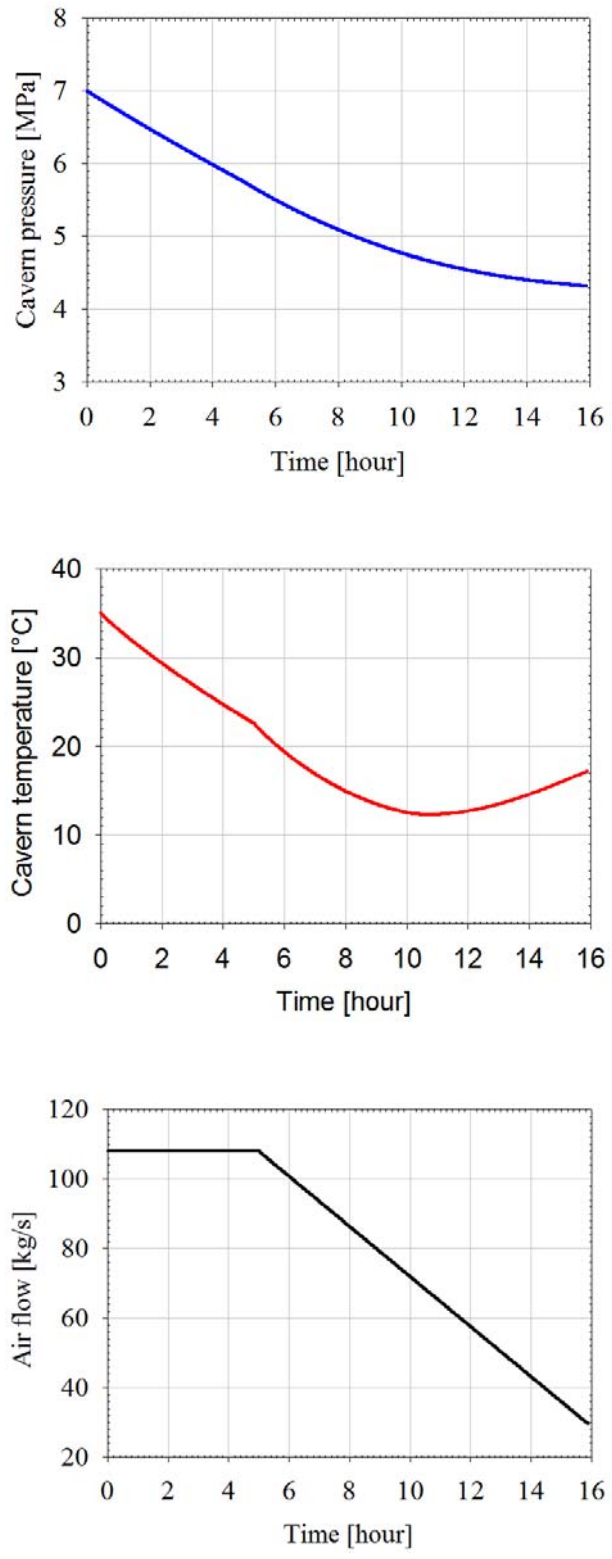

Figure 1. Compressed air storage. Gas withdrawal rate, pressure and temperature evolutions.

2.5 *Depth of penetration of temperature changes*

Solving Equation (1) allows computing temperature evolution. Brouard et al. (2011) considered a spherical cavern and applied a periodic temperature distribution at the cavern wall. They proved that accurate temperature computation requires that a refined FEM mesh be used at the vicinity of the cavern wall. The temperature distribution as a function of the distance from the cavern wall when the gas temperature is minimal is shown on Figure 2; three cycling periods are considered: one day (CAES); one week; and one month (corresponding to an "aggressively" operated HFCGSC). Even in this last case, temperature fluctuations are divided by a factor of 10 at a 3-m distance from the cavern. This distance is not strongly influenced by cavern radius.

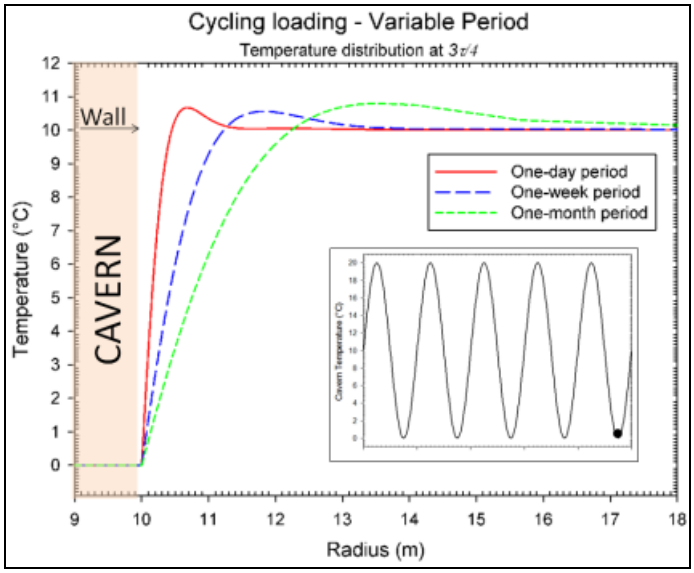

Figure 2. Temperature distribution in the rock mass after 5 cycles, when gas temperature is lowest. Cavern temperature is periodic, varying from 0 °C to 20 °C. Three periods are considered: 1 day, 1 week and 1 month. After 5 cycles, a periodic temperature evolution is reached in the rock mass (LOCAS software, Brouard et al., 2011).

3 STRESS CHANGES AT CAVERN WALL

3.1 *Thermal stresses*

Cooling (or warming) at the cavern wall generates thermal stresses. Orders of magnitudes can be computed easily. Let $\Delta T < 0$ be the difference between the rock temperature at the cavern wall and the virgin temperature (geothermal temperature) at cavern depth. Normal stresses generated by this difference are small (At the cavern wall, the thermal normal stress is zero.); however, tangential thermal stresses are of the order of $\sigma_{tt} = -E\alpha_R \Delta T / (1-\nu)$ where E = 18 GPa is the elastic modulus, ν = 0.25 is the Poisson's ratio and $\alpha_R = 4\ 10^{-5}$/°C is the thermal expansion coefficient of the rock. When $\Delta T < 0$ (gas cooling), the tangential thermal stresses are tensile, and $-\sigma_{tt} / \Delta T$ = 1 MPa/°C. This is a very high figure, tensile stresses are much larger than rock tensile strength of salt (1 to 2 MPa) and fractures open when pre-existing (compressive) stresses are not large enough.

3.2 *Example: thermal stresses at a ventilation shaft*

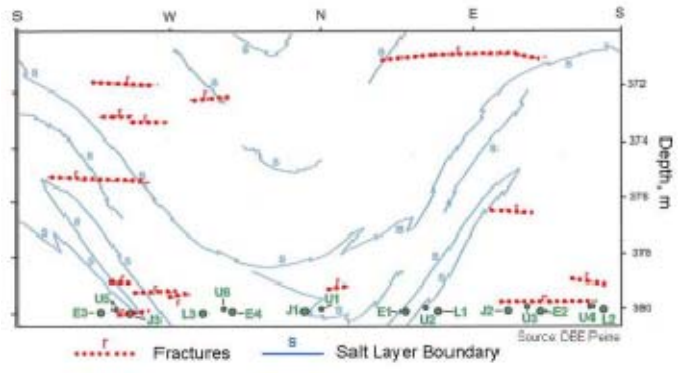

Figure 3. Gorleben Mine. Thermal fractures at the wall in a ventilation shaft. Fractures are horizontal and fractures average spacing is 2.8 m. From Zapf et al. (2012).

Wallner & Eickemeier (2001) discussed the onset of fractures in an intake air shaft of the Gorleben salt Mine in Germany. "*During the cold season, temperatures in the shaft decreased by 20°C ... within a time period of 80 days... horizontal and vertical fractures were detected by routine inspections in the shaft. Theses fractures had an average spacing of about 2.8 m. The fracture aperture amounted up to several mm."* (p. 365). This example was also discussed by Zapf et al. (2012). Rough computations explain such a phenomenon. The shaft is a cylinder, radius a. Let P_∞ be the geostatic pressure at shaft depth. It is assumed that steady-state mechanical behaviour of the rock mass can be described by a power law or $d\varepsilon/dt = A\,\sigma^n$ where n = 3 to 6. Steady-state creep closure is reached, and air temperature is cooled down by $\Delta T < 0$. At cavern wall, stresses can write (Bérest et al., 2012):

$$\begin{cases} \sigma_{rr}(a) = 0 \\ \sigma_{\theta\theta}(a) = -2P_\infty/n - E\alpha_R\Delta T/(1-\nu) \\ \sigma_{zz}(a) = -P_\infty/n - E\alpha_R\Delta T/(1-\nu) \end{cases} \qquad (3)$$

This very simple model predicts that horizontal fractures may appear when $\Delta T < -(1-\nu)P_\infty / nE\alpha_R$. At a 375-m depth, P_∞ = 8.2 MPa and, when n = 3, the condition writes ΔT < - 2.7°C, a low temperature drop (tensile strength is not taken into account).

3.3 *Spalling in gas caverns*

Is thermal fracturing a significant phenomenon in actual gas caverns? Several caverns experienced spalling, sluffing, break-outs and fast creep closure. Examples were discussed in the literature, see for instance Röhr, 1974, Baar, 1977, Serata & Cundey, 1979, Boucly & Legreneur, 1980, Coates et al., 1983, Quast, 1983, Bérest et al., 1986, Crotogino et al., 2001, Hévin et al., 2007, Rokahr et al., 2007. In most cases, these caverns were deep gas-storage caverns in which gas pressure was low when the gas inventory was small. In a gas cavern, cavern shape, cavern bottom rise and brine-gas interface rise can be measured, at least from time to time. However interpretation of these measurements often is not unequivocal; for instance, spalling *and* creep closure can both contribute to cavern bottom rise. In several cases, break-outs were observed even when pressure changes rates were relatively slow (Rokahr et al, 2007); in one case overhanging blocks fell down during the first gas injection; this may be attributed to the reduction in Archimedes thrust, when fluid density drastically drops after brine withdrawal (Quast, 1983); in this case, no or small further block fall was observed (Crotogino et al., 2001).

A characteristic example is provided by Cole (2002) who described the case of two gas caverns of the Markham storage field in Texas in which severe spalling was observed. These caverns were cycled 8 to 10 times per year. Withdrawal rates were 3-4 times faster than injection rates. Cavern tops are at 1050 m and 1075 m, and the original cavern heights were 530 m and 696 m, respectively. The first gas injections were in June 1992 (Cavern #2) and October 1995 (Cavern #5). Cavern operation resulted in cavern-volume loss and salt sluffing from the walls and roof of the cavern. Brine-gas interface surveys were run every year. As of January 2002, the caverns had lost 89 m and 128 m of their depths. A "material balance" test (the amount of withdrawn gas, pressure and temperature are carefully measured during such a test) also had been performed in 2001 to assess the cavern "free" volume, and natural gas sonar-surveys were run in January 2002. Comparison of these various methods suggests that the cavern creep closure was approximately 5% of the initial volume; however, a similar volume of salt had fallen from the walls to the bottom of the cavern. Comparison of sonar profiles proved that "*no large sections of salt from one area of the caverns fell to the bottom creating the fill ... the salt was removed in thin layers over large areas of the caverns ... horizontal cavern closure occurred ... thus closing in part of the area created by the salt falling*.", Cole, 2002, p. 82. Such features are not fully consistent with the expected effects of thermal fracturing. Munson et al. (2004) also described salt sluffing in oil storage caverns where no thermal effects can be expected. In other words, clear lessons are difficult to draw from case histories (Bérest et al., 2012).

3.4 *Fracture Mechanics*

In principle, Fracture Mechanics allow to predict the aperture, depth and spacing of thermal fractures (Nemat-Nasser et al., 1978, Bahr et al., 2010). However this domain is still a matter of researches. A few simple rules can be stated: (1) fractures are perpendicular to the cavern wall. In a cylindrical well, fractures are mostly horizontal (2) fracture depth approximately equals the depth of the zone in which tensile stresses are larger than rock tensile strength (assuming that this strength is zero is on the safe side). Obviously, the development of fractures modifies the state of stress in the vicinity of the fractures; the tensile stresses addressed here are those stresses computed with the assumption that no fracture exists.
(3) At the beginning of the cooling process, when the depth of penetration of temperature changes is shallow, stresses are tensile in a thin zone at cavern wall and many thermal micro-fractures appear at cavern wall. When low temperatures penetrate deeper into the rock mass, the propagation of many fractures stops and only a small number of them continue to grow. This process is illustrated in Figure 4. (4) The ratio between fractures depth and fractures spacing is not very different from 1. (5) The ratio between the fracture aperture, or o, and fracture spacing, or s, typically is $o/s = -\alpha_R \Delta T$ ($\Delta T < 0$ is the temperature change at the cavern wall). In the case of the Gorleben shaft (section 3.2), ΔT = - 20°C, α_R = 4 10^{-5}/°C, s = 2.8 m and fracture aperture can be expected to be o = 2 mm or so.

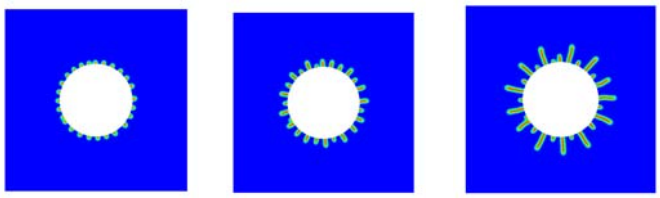

Figure 4. Onset of fractures at a cylindrical cavern wall. A -5 °C temperature drop is applied at the cavern wall and kept constant. From left to right: After some time, fractures appear at the cavern wall. As the cold temperature front penetrates deeper into the rock mass, a smaller number of fractures keep growing (Sicsic et al., 2013).

3.5 *Effective tensile stresses*

It was assumed that fractures can appear when a tangential tensile stress develops at the cavern wall. (The effect of gas pressure was not taken into account.) However, this criterion may be too optimistic. When performing a hydraulic fracturing test in a borehole, fluid pressure in the borehole is increased to a figure slightly higher than the geostatic pressure to create a fracture. Such tests are performed routinely to assess in-situ stresses. When interpreting such tests, one must take into account the onset of *effective* tensile stresses. Effective stresses are the sum of the actual stresses (compressive are negative) plus the fluid pressure. When the least stress is tensile (positive), the onset of fracturing is possible. This criterion is more severe than the no-tensile-stress criterion considered above. Whether such a criterion ("no effective tensile stress") must be taken into account is still open to discussion (Brouard et al., 2007).

4 CONCLUSIONS

The thickness of the zone at cavern wall in which stresses are tensile can be computed through standard numerical computations. Generally speaking, this zone is not very thick as gas never remains much colder than the rock mass during a very long period of time. There is no significant risk of block fall, as the blocks delimited by two consecutive fractures remain strongly bounded to the rock mass (Pellizzaro et al., 2011). However some specific zones (such as non-convex parts of the cavern profile, or flat roofs whose span is large) are more prone to develop tensile stresses and can be subject to spalling, leading to a smoother profile of the cavern. They are not a real concern. Cavern tightness also must be considered. The distance between cavern top and salt roof must be significantly larger than the thickness of the possible tensile zone. Simple numerical com-putations allow checking that this criterion is met.

5 ACKNOWLEDGEMENTS

This study was funded partially by the French Agence Nationale de la Recherche (ANR) in the framework of the SACRE Project, which includes researchers from EDF, GEOSTOCK, PROMES (Perpignan), HEI (Lille) and Ecole Polytechnique (Palaiseau).

6 REFERENCES

ATG. 1986. Stockages souterrains de gaz (Underground gas storages). Manuel pour le transport et la distribution du gaz, Titre XIII. *Association technique de l'industrie du gaz en France, 62 rue de Courcelles, 75008 Paris France* (In French).

Baar, C.A. 1977. *Applied salt-rock mechanics. Vol. I.* Developments in Geotechnical Engineering. 16-A. Amsterdam: Elsevier Science.

Bahr H.A., Weiss H.J., Bahr U., Hoffmann M., Fischer G., Lamperscherf S. & Balke H. 2010. Scaling behavior of thermal drying. J. Mech. Ph. Solids 58 (2010): 1411-1421.

Bérest P., Ghoreychi M., Fauveau M., & Lebitoux P. 1986. Mechanism of Creep in Gas storage Caverns. Effect of gravity forces. *27th US Symp on Rock Mech*. Hartman H.L. ed., soc. Min. Eng. Inc., Littleton, Colorado: 789-794.

Bérest P., Djizanne H., Brouard B. & Hévin G. 2012. Rapid depressurizations: can they lead to irreversible damage? *SMRI Fall Meeting, Regina*: 64-83.

Boucly Ph. & Legreneur J. 1980. Hydrocarbon storage in cavities leached out of salt formations. *Int. Symp. Subsurface Space, Stockholm, Sweden*: 251-257.

Brouard B., Karimi-Jafari M. & Bérest P. 2007. Onset of Tensile effective Stresses in Gas Storage Caverns. *SMRI Fall Meeting, Halifax, Canada:* 119-135.

Brouard B., Frangi A. & Bérest P. 2011. Mechanical stability of a cavern submitted to high-frequency cycles. *SMRI Spring Meeting, Galveston, Texas:* 99-116.

Coates G.K., Lee C.A., McLain W.C. & Senseny P.E. 1983. Closure and Collapse of Man-Made Cavities in Salt. *Proc. 6th Int. Symp. Salt*: 139-157.

Cole R. 2002. The long Term Effects of High Pressure Natural Gas Storage on Salt Caverns. *SMRI Spring Meeting, Banff, Canada:* 75-97.

Crossley N.G. 1996. Salt cavern Integrity Evaluation Using Downhole Probes. A Transgas Perspective. *SMRI Fall Meeting, Cleveland, Ohio:* 21-54.

Crotogino F., Mohmeyer K.U, & Scharf R. 2001. Huntorf CAES: More than 20 Years of Successful Operation. S*MRI Spring Meeting, Orlando, Florida:* 351-362

Fosse A.P. & Røvang L.B. 1998. Verifying Established Initial Gas Temperature Distribution in Caverns. *SMRI Spring Meeting, New Orleans, Louisiana*: 126-142.

Hévin G., Caligaris C., Durup & J.G. 2007. Deep salt cavern abandonment: a pilot experiment. *SMRI Fall Meeting, Halifax, Canada*: 16-25.

Klafki M., Wagler T., Grosswig S. & Kneer A. 2003. Long-term downhole fibre optic temperature measurements and CFD modeling for investigation of different gas operating modes. *SMRI Fall Meeting, Chester, UK:* 180-189.

Kneer A. Irmer A., Riegel H. & Klafki M. 2002. Application of a CFD-Code for Modeling of 3-D Processes in salt Caverns during Gas Withdrawal. *SMRI Fall Meeting, Bad Ischl, Austria:* 197-209.

Krieter M., Hagoort J. & Barnewold D. 1998. Thermodynamic Simulation of Gas Caverns for Optimized Production Management. *SMRI Fall Meeting, Roma*: 309-325.

Krieter M. 2011. Influence of gas cavern's surface area on thermodynamic behaviour and operation. *SMRI Fall Meeting, York, UK:* 179-184.

Munson D.E., Ehgartner B., Bauer S., Rautman C. & Myers R. 2004. Analysis of a salt fall in Big Hill Cavern 103, and a preliminary concept of salt dome structure. *SMRI Spring Meeting, Wichita, Kansas:* 57-72.

Nemat-Nasser S., Keer L.M. & PanharK.S. 1978. Unstable growth of thermally induced interacting cracks in brittle solids. Int. J. Solids Struct. 14: 409-430.

Pellizzaro C., Bergeret G., Leadbetter A. & Charnavel Y. 2011. Thermomechanical behavior of Stublach Gas Storage Caverns. SMRI Fall Meeting, York, UK : 161-178.

Quast P. 1983. L'installation de Huntorf : plus de trois années de fonctionnement de cavernes à air comprimé. Annales des Mines, 190ème année, n°5-6, mai-juin 1983 : 93-102. (In French)

Röhr H.U. 1974. Mechanical behavior of a gas storage cavern in evaporitic rocks. Proc. 4th Symp. on Salt, A.H. Coogan ed., Salt Institute, II: 93-100.

Rokahr R., Staudtmeister K., Zander-Schiebenhöfer D. & JohansenJ.I. 2007. In-situ Test with a Gas Storage Cavern as a Basis for Optimization. SMRI Spring Meeting, Basel, Switzerland: 84-97.

Serata S. & Cundey T.E. 1979. Design Variables in Solution Cavities for Storage of Solids, Liquids and Gases. Proc. 5th Symposium on Salt, The Northern Ohio Geological Society Inc. Pub.,:161-170.

Sicsic P., Marigo J.J. & Maurini C. 2013. Initiation of a periodic array of cracks in the thermal shock problem: a gradient damage modeling. Submitted to J.Mech.Ph.Solids.

Skaug N., Ratigan J. & Thompson M. 2010. Natural Gas Cav ern Inventory Assessment — A new approach. *SMRI Spring Meeting, Gd Junction, Colorado*: 303-312.

Wallner M. & Eickemeier R. (2001) – Subsidence and Fractures Caused by Thermo-Mechanical Effects. *SMRI Spring Meeting, Orlando, Florida*: 363-371.

Zapf D. Staudtmeister K., & Rokahr R.B. 2012. Analysis of thermal induced fractures in salt. *SMRI Spring Meeting, Regina, Saskatchewan:* 47-62.